Lattice Gauge Theories: a numerical exercise

Andrea Coser

September 3, 2012

Introduction

Gauge theories are supposed to rule the fundamental interactions in our actual description of Elementary Particles. The requirement of a local symmetry (the symmetry transformations depend on space-time coordinates), forces us to introduce new particles, the gauge vector bosons, which carry the interaction between the other matter particles (the scalar bosons and the spin 1/2 fermions).

The simplest gauge theory which one can think of is the Abelian $U(1)$ gauge theory, which has been widely studied with the help of perturbation theory. The Renormalization Group (RG) improved running coupling constant is found to be small in the low energy regime and therefore the theory is suitable for perturbation theory. It describes Quantum Electrodynamics (QED) with outstanding precision, but it was found useless to describe the strong interactions. Indeed, it predicts free charged states (as for example electrons and positrons) and long range interactions, while for strong forces colored free states (like free quarks) have never been found and the interaction is found to be short-ranged (the range of the interaction is of the order of the femtometer, the dimension of the nuclei).

The introduction of non-Abelian gauge theories elegantly overcomes these problems: the RG investigation indeed reveals that the conclusions drawn for the $U(1)$ case are not valid any more. Non-Abelian gauge theories are intrinsically more difficult to study since perturbation theory cannot be used to understand the behavior of strong forces in the low energy regime. Non-Abelian gauge theories experience the so-called asymptotic freedom: the running coupling constant tends to zero in the high energy regime and in this situation experiments are well described by the results of perturbation theory. In sufficiently high energy collisions, the quarks which protons and other hadrons are made of, act more or less as if they were free. However, in the infrared (IR) regime the RG flow is not trivial and perturbation theory cannot be applied.

A great effort has been done to find a new approach to study this regime and to see if the theory actually predicts as fundamental states colorless bound states and the interaction is confined inside these bound states. This is not trivial at all and, apart from some non-perturbative results, the only practicable way is to set up a numerical computation. Since computers work only with finite quantities, when we set up a simulation we need to discretize space-time. The simplest way to do this is to put the theory on a (hypercubic) lattice. In this way we manually introduce an ultraviolet (UV) regularizator, the lattice

spacing a. Since we can only deal with finite lattices, we also introduce an IR regularizator, the lattice dimension L (we can consider different dimensions in the space and time directions).

When we introduce the UV cutoff a we need to pick up a theory whose trivial continuum limit $a \to 0$ reproduces the initial gauge theory originally defined in the continuum. However, the choice of such a regularized theory is not unique, and a naive discretization sometimes turns out to be impossible (as in the very important case in which one introduces dynamical quarks). Once the theory has been correctly discretized and the physics on the lattice has been studied, it is then necessary to take the continuum limit in order to obtain results on the continuum physics. This is a non-trivial task, both from the theoretical and the computational point of view since it requires RG calculations and a high computational effort. In principle one should also take an infinite lattice limit or at least study finite size effects by varying the lattice dimensions. This again requires very long computational time.

For this exercise, I studied the general theory of lattice gauge theories and how to apply it to set up a simple numerical computation. I restrict myself to the study of pure gauge theories, that is of theories with only the gauge field, without the fermionic content. Both Abelian and non-Abelian lattice gauge theories were taken under examination and the continuum limit was studied in the limit of the available computational power. The non-zero temperature case is also briefly discussed.

In sec. 1 we will review the basic concepts of lattice gauge theories, in sec. 2 we will discuss the numerical techniques used and finally in sec. 3 we will present the results obtained and compare them with the known ones.

1 Gauge Theories on the Lattice

1.1 Gauge theories in the continuum

Let us consider the action of a single free spin-1/2 massive fermion (a quark) in d spacetime dimensions (from now on, all the analysis will be performed considering imaginary euclidean time):

$$S_F[\psi, \bar{\psi}] = \int \mathrm{d}^d x \, \bar{\psi} \left(\gamma_\mu \partial_\mu + m\right) \psi \,. \tag{1}$$

Here ψ is a Dirac four-component spinor and γ_μ are the Dirac matrices satisfying the Clifford algebra $\{\gamma_\mu, \gamma_\nu\} = 2\delta_{\mu\nu}\mathbb{I}$. We now want to introduce the gauge interaction. First of all we consider N of such fermions labeled by the index A (color) and we notice that the resulting theory is invariant under the global action of the group $SU(N)$

$$\psi_A(x) \to \Omega_{AB}\psi_B(x) \,, \qquad \bar{\psi}_A(x) \to \bar{\psi}_B(x)(\Omega^\dagger)_{BA} \,. \tag{2}$$

From now on, we will use matrix notation, without explicitly writing the color indices. When we promote the action of $SU(N)$ to be local, the presence of the derivative term will spoil the symmetry. We are forced to introduce a new bosonic vector field to compensate and restore the symmetry. The following Lagrangian:

$$S_F[\psi, \bar{\psi}] = \int \mathrm{d}^d x \, \bar{\psi} \left(\gamma_\mu (\partial_\mu + igA_\mu(x)) + m\right) \psi \,, \tag{3}$$

is invariant under local (space-time dependent) gauge transformations

$$\begin{aligned} &\psi(x) \to \Omega(x)\psi(x)\,, \qquad\qquad \bar{\psi}(x) \to \bar{\psi}(x)\Omega^\dagger(x)\,, \\ &A_\mu(x) \to \Omega(x)A_\mu(x)\Omega(x)^\dagger + \frac{i}{g}\left(\partial_\mu\Omega(x)\right)\Omega(x)^\dagger\,. \end{aligned} \tag{4}$$

Here the gauge field $A_\mu(x)$ are $N \times N$ hermitian traceless matrices and the factor g is the (bare) interaction parameter. We finally introduce a term which describes the free propagation and the self-interaction of the gauge boson. The only renormalizable, gauge invariant term is the following:

$$\begin{aligned} &S_G[A_\mu] = \frac{1}{2}\int \mathrm{d}^d x\, \mathrm{Tr}\left[F_{\mu\nu}(x)F_{\mu\nu}(x)\right]\,, \\ &F_{\mu\nu}(x) = \partial_\mu A_\nu(x) - \partial_\nu A_\mu(x) + ig\left[A_\mu(x), A_\nu(x)\right]\,. \end{aligned} \tag{5}$$

The quantity $F_{\mu\nu}(x)$ is called the field strength. Any constant factor in front of S_G may be reabsorbed in the constant g.

The gauge field $A_\mu(x)$ is hermitian and traceless and the gauge transformation preserves these characteristics. Therefore it is an element of the Lie algebra $su(N)$ and can be parametrized using the algebra generators

$$A_\mu(x) = \sum_{a=1}^{N} A_\mu^a(x) T^a\,. \tag{6}$$

The fields strength too, can be represented in the same way and a simple calculation reveals that

$$\begin{aligned} &F_{\mu\nu}(x) = \sum_{a=1}^{N} F_{\mu\nu}^a(x) T^a\,, \\ &F_{\mu\nu}^a(x) = \partial_\mu A_\nu^a(x) - \partial_\nu A_\mu^a(x) - g f^{abc} A_\mu^b(x) A_\nu^c(x)\,, \end{aligned} \tag{7}$$

where the f^{abc} are the structure constants of the Lie algebra $su(N)$. The last term of eq. (7) clearly shows the presence of self-interaction of the gauge field. These terms are not present in the Abelian case and are responsible for confinement of color. They also make pure gauge theories highly nontrivial.

1.2 Discretization of gauge theories

As already discussed, to perform a numerical study we need to regularize the theory by discretizing space-time. We consider a lattice $\Lambda = \{n = (n_0, \vec{n}) \,|\, n_0 = 0, \ldots, N_t - 1;\, n_i = 0, \ldots, N-1\}$ with lattice spacing a and we denote with $\hat{\mu}$, $\mu = 1, \ldots, d$ the fundamental vectors on such a lattice. We place the fermionic degrees of freedom on the sites of such a lattice, $\psi(n)$, $\bar{\psi}(n)$, $n \in \Lambda$. The action for a free fermion on the lattice may be written

as follows[1]:

$$S_F[\psi,\bar{\psi}] = a^d \sum_{n\in\Lambda} \bar{\psi}(n) \left(\sum_{\mu=1}^{d} \gamma_\mu \frac{1}{2a} \left(\psi(n+\hat{\mu}) - \psi(n-\hat{\mu})\right) + m\,\psi(n) \right) . \tag{8}$$

Here the integral is replaced with a sum over the lattice sites (the dimension is recovered with the help of the dimensionful lattice constant a), while the derivative is replaced by its discretized version.

The gauge transformations act again as a rotation of the color indices of the quark field. On the lattice we choose an $SU(3)$ matrix for each lattice site $n \in \Lambda$

$$\psi(n) \to \Omega(n)\psi(n)\,, \qquad\qquad \bar{\psi}(n) \to \bar{\psi}(n)\Omega^\dagger(n)\,. \tag{9}$$

Again we are forced to introduce the gauge field in order to restore the symmetry of the derivative term in the action. The gauge variables are placed on the links of the lattice and they possess an intrinsic orientation. The field $U_\mu(n)$ is on the lattice link between site n and site $n+\hat{\mu}$ pointing in the $\hat{\mu}$ direction. The link variable $U_{-\mu}(n)$, however, is not independent since $U_{-\mu}(n) = U_\mu(n-\hat{\mu})^\dagger$. The gauge transformations act on the link variables as follows:

$$\begin{aligned} U_\mu(n) &\to U'_\mu(n) = \Omega(n) U_\mu(n) \Omega(n+\hat{\mu})^\dagger\,, \\ U_{-\mu}(n) &\to U'_{-\mu}(n) = \Omega(n) U_{-\mu}(n) \Omega(n-\hat{\mu})^\dagger\,. \end{aligned} \tag{10}$$

The following action is invariant under this set of transformations

$$S_F[\psi,\bar{\psi},U] = a^d \sum_{n\in\Lambda} \bar{\psi}(n) \left(\sum_{\mu=1}^{d} \gamma_\mu \frac{1}{2a} \left(U_\mu(n)\psi(n+\hat{\mu}) - U_{-\mu}(n)\psi(n-\hat{\mu})\right) + m\,\psi(n) \right) . \tag{11}$$

Notice that we can formally recover the continuum action by introducing the algebra-valued lattice gauge fields $A_\mu(n)$ through $U_\mu(n) = \exp(iaA_\mu(x))$, expanding to order a and taking the naive limit $a \to 0$. This is a minimal requirement, but it is not enough, as already discussed. However, ignoring more subtle issues, we can already see that the link variable is essentially the lattice version of the gauge transporter (path-ordered exponential integral of the gauge field A_μ) from site n to site $n+\hat{\mu}$. When we replace $U_\mu(n)$ with $\exp(iaA_\mu(x))$ we are actually approximating the integral along the path between n and $n+\hat{\mu}$ with $aA_\mu(x)$. This approximation is valid at order $\mathcal{O}(a)$. The link variables $U_\mu(n)$ are group variables and can be taken as fundamental objects which are integrated over in the path integral. These variables turn out to be particularly suitable for the lattice computation.

1.3 The Wilson action

Consider an ordered path $\mathcal{P}$ in the lattice starting from n_0 and ending in n_1. Consider then the ordered product of the link variables along this path $\prod_{(n,\mu)\in\mathcal{P}} U_\mu(n)$. Under a

[1] Actually, after a closer look, this naive discretization is found to be wrong. Even if in the naive continuum limit $a \to 0$ we actually recover the correct continuum action, if we compute the propagator in this lattice description we would find many poles representing spurious particles, not present in the original continuum formulation. This problem can be overcome using a more clever discretization, however we will not exploit the details of this procedure, since the numerical study will involve only a pure gauge theory.

gauge transformation this object will transform as

$$\prod_{(n,\mu)\in\mathcal{P}} U_\mu(n) \to \Omega(n_0) \left[\prod_{(n,\mu)\in\mathcal{P}} U_\mu(n) \right] \Omega(n_1)^\dagger \,. \tag{12}$$

All the other gauge matrices along the path cancel out and the only left are the ones corresponding to the initial and final site. It is clear now that the trace of a product around a closed loop $\mathcal{L}$ is a gauge invariant quantity[2]. Such an object is called a Wilson loop

$$W[U] = \mathrm{Tr} \prod_{(n,\mu)\in\mathcal{L}} U_\mu(n) \,. \tag{13}$$

The shortest, more fundamental Wilson loop is defined along a single plaquette

$$\begin{aligned} U_{\mu\nu}(n) &= U_\mu(n) U_\nu(n+\hat{\mu}) U_{-\mu}(n+\hat{\mu}+\hat{\nu}) U_{-\nu}(n+\hat{\nu}) \\ &= U_\mu(n) U_\nu(n+\hat{\mu}) U_\mu(n+\hat{\nu})^\dagger U_\nu(n)^\dagger \,. \end{aligned} \tag{14}$$

Using plaquette variables we can build the pure gauge action

$$S_G[U] = \frac{2}{g^2} \sum_{n\in\Lambda} \sum_{\mu<\nu} \mathrm{Re}\,\mathrm{Tr}\left[\mathbb{I} - U_{\mu\nu}(n)\right] \,. \tag{15}$$

This form of the action is known as the Wilson action. As before, it is easy to show that in the naive continuum limit $a \to 0$ this expression gives back the usual pure gauge action, eq. (5).

With the pure gauge and the fermionic action that we introduced in this section, we can write the (Euclidean) correlator of any observables O_1 and O_2 as a path integral

$$\begin{aligned} \langle O_2(t) O_1(0) \rangle &= \frac{1}{Z} \int \mathcal{D}[\psi,\bar{\psi}]\mathcal{D}U \, O_2[\psi,\bar{\psi},U;t] O_1[\psi,\bar{\psi},U;0] \, e^{-S_F[\psi,\bar{\psi},U]-S_G[U]} \,, \\ Z &= \int \mathcal{D}[\psi,\bar{\psi}]\mathcal{D}U \, e^{-S_F[\psi,\bar{\psi},U]-S_G[U]} \,. \end{aligned} \tag{16}$$

The fact that we can define the theory through this path integral is fundamental for the numerical study. In this way we can set up a Monte Carlo simulation treating the (euclidean) path integral as the partition function of a d-dimensional statistical system.

1.4 Wilson loops, Polyakov loops and the static $q\bar{q}$ potential

We already defined the Wilson loops in eq. (13), we now want to give the physical interpretation of such quantities. We will consider a rectangular Wilson loop embedded in a fundamental plane of the lattice containing the temporal direction. This loop is therefore made of two temporal transporters $T(\vec{n}, n_t)$, $T(\vec{m}, n_t)$ and two spatial transporters

[2] This is not the only possibility. Another gauge invariant quantity can be constructed attaching a fermion and its antiparticle at the end and at the beginning of the path. We are now interested in pure gauge object in order to build the pure gauge action.

$S(\vec{m},\vec{n};0)$, $S(\vec{m},\vec{n};n_t)$. With a suitable gauge transformation it is possible to fix all the link variables along the temporal transporters to the identity $\mathbb{I}$

$$\langle W[U]\rangle = \langle \mathrm{Tr}[S(\vec{m},\vec{n};0)S(\vec{m},\vec{n};n_t)^\dagger]\rangle \,. \tag{17}$$

For large extent of the spatial direction of the lattice T, this correlator can be expressed in terms of the Hilbert space states and operators (here denoted with a hat) as

$$\langle \mathrm{Tr}[S(\vec{m},\vec{n};0)S(\vec{m},\vec{n};n_t)^\dagger]\rangle = \sum_k \langle 0|\hat{S}(\vec{m},\vec{n})|k\rangle\langle k|\hat{S}(\vec{m},\vec{n})^\dagger|0\rangle e^{-tE_k} \,. \tag{18}$$

It is possible to argue that the states $|k\rangle$ with non-vanishing overlap on the state $S(m,n)^\dagger|0\rangle$ are states which contain a static quark-antiquark pair located at sites $\vec{n}$ and $\vec{m}$. The lowest eigenenergy E_0 will therefore correspond to the static potential $V(r)$ between the $q\bar{q}$ pair at a distance $r = |\vec{n}-\vec{m}|$. Higher energy states will correspond to more complicated states, for example containing additional particle-antiparticle pairs generated by vacuum polarization effects. The contribution of these states to the propagator and therefore to the Wilson loop is suppressed by an exponential factor $e^{-n_t a \Delta E}$, with $\Delta E = E_k - E_0$. Therefore, for sufficiently high values of n_t, we should be able to extract the static potential from the average value of the Wilson loops. With this considerations we can understand that it is possible to have an important evidence of confinement even within the pure gauge theory, without introducing dynamical fermions.

Another important gauge invariant quantity is the Polyakov loop. If we consider periodic boundary conditions in the time direction of our lattice we can consider a Wilson loop made by a single time transporter that winds around the time direction. When we take the trace we again have a gauge invariant quantity. Such a loop is called a Polyakov loop

$$P(\vec{m}) = \mathrm{Tr}\left[\prod_{j=0}^{N_t-1} U_0(j,\vec{m})\right] \,. \tag{19}$$

If we consider two Polyakov loops at positions $\vec{n}$ and $\vec{m}$ with opposite orientations, and we go in the particular gauge in which the link variables of the spatial transporter connecting $(\vec{n},0)$ and $(\vec{m},0)$ are set to unity, then it is clear that the product of the two Polyakov loops corresponds to the Wilson loop with time extension equal to the full time extension. Since Polyakov loops and Wilson loops are gauge invariant, it is clear that Polyakov loops can as well used to extract the static $q\bar{q}$ potential. Polyakov loops are also important in the case of non-zero temperature, that we will discuss in the following.

We are interested in the nature of the static potential $V(r)$ to understand if the theory shows confinement. We can get some information on $V(r)$ by performing strong and weak coupling expansions. It actually turns out that on the lattice it is much easier to perform a strong coupling expansion and it is relatively simple to see that in this regime the static potential is linear in the distance r

$$V(r) \underset{g\to\infty}{\sim} \sigma r \,, \tag{20}$$

with some constant σ, sometimes called the *string tension*. On the contrary, when $g \to 0$, the self interaction of the gauge field is less and less important (see eq. (7)) and therefore

we expect the static potential to get closer to the one of QED, that is the electric potential $\sim 1/r$. With these considerations in mind, we can parametrize $V(r)$ as follows

$$V(r) = A + \frac{B}{r} + \sigma r \,. \tag{21}$$

Notice that if σ is different from zero, when we try to separate our two static quarks the potential between then grows and it finally diverges when we put the two color charges at infinite distance. This is of course unphysical: in real world, when dynamical quarks are separated far apart and the potential between them increases, the creation of new $q\bar{q}$ pairs from the vacuum will be energetically favorable, these new quarks will screen the gauge potential and new bound states will be created (this process is the base of hadronization). Nevertheless, σ can be considered as an order parameter[3] to describe the confining and non-confining phase of the lattice theory. The string tension σ will be the main object of our numerical investigation.

1.5 Renormalization Group and the continuum limit

We constructed a lattice gauge theory which in the naive continuum limit $a \to 0$ reproduces the correct continuum gauge theory. This is not the only possible construction and we just chose the simplest one. However, it is still not clear if the continuum limit of such theories exists and is indeed a gauge invariant field theory.

A first requirement is that in the continuum the quark masses (that we generally call m) must be finite. The lightest mass is related to the inverse of the largest correlation length of the theory on the lattice. If we denote with a hat the dimensionless quantities on the lattice, we realize that

$$\hat{\xi}^{-1} \sim \hat{m} = m\, a \xrightarrow[a\to 0]{} 0 \,, \tag{22}$$

that is the continuum limit emerges as a critical region of the lattice theory, where the (dimensionless) correlation length diverges. Indeed, at a critical point the system looses memory of the underlying lattice structure. To reach the critical point we must tune the parameters of the theory. In the pure gauge formulation only one parameter is present, the bare coupling g (which is void of any physical meaning), and it must be tuned to a critical value $g_\star$ to obtain a diverging correlation length. Therefore, while shrinking the lattice spacing we must tune the bare parameter in order to obtain a critical lattice theory and finite physical quantities.

For a dimensionful observable O, with mass dimension d_O, we denote with $\hat{O}$ its dimensionless lattice counterpart, which will depend on the bare coupling and can be computed numerically form a lattice simulation

$$O(g,a) = \left(\frac{1}{a}\right)^{d_O} \hat{O}(g) \,. \tag{23}$$

Requiring that the lhs approaches a physical finite limit for small lattice spacing

$$O(g(a),a) \xrightarrow[a\to 0]{} O_{\text{phys}} \,, \tag{24}$$

[3]Notice that σ is a non-local order parameter, since it is built from non-local objects, such as Wilson or Polyakov loops. Elitzur theorem [1] indeed rules out the possibility of transitions with local order parameters in any lattice gauge theory.

we can determine $g(a)$. This functional dependence should be universal for sufficiently small lattice spacing a in order to allow for all observables to be finite. We can determine the function $g(a)$ setting up a Callan-Symanzik equation and then applying perturbation theory expanding the beta-function around $g = 0$. The requirement of finite physical observables, eq. (24), reads for small a

$$\frac{\mathrm{d}O}{\mathrm{d}\ln a}(g(a), a) = 0\,, \qquad \left(\frac{\partial}{\partial \ln a} + \frac{\partial g}{\partial \ln a}\frac{\partial}{\partial g}\right) O(g(a), a) = 0. \tag{25}$$

Perturbation theory gives for a $SU(N)$ pure gauge theory (with dynamical fermions we would find terms proportional to the number of quark flavors)

$$\begin{aligned} \beta(g) \equiv -\frac{\partial g}{\partial \ln a} &= -\beta_0 g^3 - \beta_1 g^5 + \mathcal{O}(g^7)\,, \\ \beta_0 &= \frac{1}{(4\pi)^2}\frac{11}{3}N\,, \\ \beta_1 &= \frac{1}{(4\pi)^4}\frac{34}{3}N^2\,. \end{aligned} \tag{26}$$

From the last equation we see that since $\beta(g)$ is negative in the small coupling region, the RG flow will bring g close to the fixed point $g_\star = 0$. Therefore the continuum limit corresponds to vanishing bare coupling. This fact is called asymptotic freedom. Integrating the beta function we can find the relation between g and a up to this order

$$a(g) = \frac{1}{\Lambda_L} R(g) = \frac{1}{\Lambda_L}(\beta_0\, g^2)^{-\frac{\beta_1}{2\beta_0^2}} \exp\left(-\frac{1}{2\beta_0 g^2}\right)\,. \tag{27}$$

Here Λ_L is an integration constant and it is used to set the scale by fixing the value of g at some a. The scale Λ_L is a physical scale in term of which physical quantities can be measured[4], in contrast with the non-physical lattice spacing a, introduced only as a possible regularization of the theory.

Using eq. (27) in eq. (23) we can see that

$$\hat{O}(g) \underset{g\to 0}{\sim} \hat{C}_O (R(g))^{d_O}\,, \tag{28}$$

where $\hat{C}_O$ is a dimensionless constant. In the numerical simulation we can study $\hat{O}(g)$ as function of the bare parameter, looking for this kind of scaling behavior. In general we expect the scaling region to be close to $g_\star = 0$. However, for too small values of the bare parameter the lattice spacing a will also be very small and the finite lattice used for the numerics will actually correspond to a very small real space sample, smaller than the typical scale of the physics we are interested in. Therefore the calculation will suffer of severe finite size effects. In conclusion, on a finite lattice and varying the bare parameter, we expect to find a scaling window where the behavior of the observables is well described by eq. (28). Using eq. (24) we can relate the physical observables to the dimensionless quantities measured in the scaling window

$$O_{\mathrm{phys}} = \hat{C}_O\, \Lambda_L^{d_O}\,. \tag{29}$$

[4]The scale Λ_L can be related to the famous Λ_{QCD} and it plays the same role.

This means that performing a numerical calculation physical quantities can be measured in terms of the physical scale Λ_L, which must be determined by comparing the numerical results with the experiments.

One can also study the continuum limit by varying the number of lattice sites and the couping accordingly, following eq. (27), thus keeping the physical lattice size constant. One can study just a few values of the coupling constant, since decreasing g the number of lattice sites quickly becomes prohibitive. One should then perform an extrapolation to $g = 0$. Finally in principle one should also perform an infinite space-time limit, by studying the system for different physical dimensions,

2 The numerical computation

2.1 Structure of the program

The program that was used to simulate the pure gauge theory on the lattice has a very simple structure. The main object is the lattice, and the gauge variables are set on its links: for $SU(2)$ and $SU(3)$, the link variables are represented by the usual 2×2 and 3×3 unitary matrix representations, while for the $U(1)$ gauge group unitary complex numbers where used and for the Z_n group just an integer number representing the discrete phase was stored.

The aim of the program is to compute average values or correlators of the form of eq. (16). These kinds of integrals can be computed using a Monte Carlo technique, generating lattice configurations distributed according to the probability distribution function (pdf) $\exp(-S_G[U])$ and computing averages and correlators as the arithmetic averages over these sampled configurations. Since it is in general not possible to generate configurations distributed according to a generic pdf, the class of Monte Carlo methods provide a way to set a Markov chain in the space of configurations. The Markov process will end in an equilibrium distribution where averages are computed on. The Markov chain must be set such that it efficiently has access to the whole configuration space, visiting more often the most probable configurations. This ergodicity requirement may be a problem if configuration space is split in two or more topologically different sectors, as for example if a spontaneous symmetry breaking is present.

The main function of the program will start with the initialization of the system to a certain configuration. It may be "cold", if all link variables are set to unity, "hot" if the group elements are chosen at random, or a mixed configuration. After the initialization, a loop over a certain amount of Monte Carlo iterations is performed in order to make the system reach the equilibrium configuration (thermalization). To understand when the system is thermalized, the relaxation of the average value of some simple observables (like the action) has been studied. Different initializations are taken into account and when the chosen observables relax to a common value for both hot and cold start, the system is considered in equilibrium.

After thermalization, observables can be measured. Another loop of Monte Carlo steps is performed: at each step the lattice configuration is updated and subsequently the observable is computed on the new configuration. The final estimator of the observable

will be the average over all the measurements along the Markov chain.

The error has been computed as the estimator of the statistic error for uncorrelated random variables. This actually severely underestimates the error, since any configuration depends on the previous one along the chain and therefore they are correlated. One should study the correlation time (here I mean computer time) after which two configurations can be considered independent and modify the error estimation accordingly. In order to partially cure the problems due to correlation, since the computation of observables is very time consuming, one can perform more than one Monte Carlo updates before each measurement. In this way subsequent configurations with measurements will be less correlated. How to decide how many of these updates without measurements may be performed is a matter of choice. A better decision may be taken by studying the correlation time of the Markov chain.

2.2 Link variable storage

A large part of the simulation time is spent multiplying the gauge group link variables, therefore it turns out to be more convenient to loose efficiency in storing the link variables while decreasing the computational effort of group elements multiplication

$U(1)$**:** group elements are stored with real and imaginary parts, instead of a single real phase, in order to avoid the use of sin and cos functions.

$SU(2)$**:** four real elements are stored instead of three according to the decompositions in term of Pauli matrices

$$U = a_0 \mathbb{I} + i\, \vec{a} \cdot \vec{\sigma}\,, \tag{30}$$

with $a_0^2 + |\vec{a}|^2 = 1$.

$SU(3)$**:** the gauge group has eight independent parameters, however twelve real numbers are stored, corresponding to the first two rows of the unitary 3×3 matrix. The third row is constructed from the first two according to

$$U = \begin{pmatrix} \vec{u} \\ \vec{v} \\ \vec{u}^* \times \vec{v}^* \end{pmatrix}. \tag{31}$$

The vectors $\vec{u}$ and $\vec{v}$ must be normalized to unity and mutually perpendicular, thus ensuring that these properties will be shared by the vector of the third raw, too.

Z_n**:** the group elements are stored as integer numbers corresponding to the fraction of the unit circle of the corresponding root of unity.

Except for the case of Z_n, after some computations, due to accumulation of rounding errors in multiplying group elements, the gauge matrices could be not unitary any more. The link elements must therefore be regularly projected to unitarity.

2.3 The Metropolis algorithm

The Monte Carlo updates have been performed (except for the $SU(2)$ and Z_2 case, see next section) using a simple Metropolis algorithm, by proposing and testing a new link variable subsequently for one link at a time. A Monte Carlo step was completed after testing all sites in the lattice. When testing a single link variable $U_\mu(n)$, a new candidate is proposed $U_\mu(n)'$. If the new total action is equal or less than the previous one, the new candidate is accepted with probability one, otherwise it is accepted with probability $\exp(-\Delta S)$. This procedure assures that the transition probabilities in the space of lattice configurations will satisfy detailed balance and therefore an equilibrium solution must exist and it is the desired one.

On a hypercubic lattice in d spacetime dimensions, each link is shared by $2(d-1)$ plaquettes. The local contribution of the action which contain the contribution of a single link is given by

$$S[U_\mu(n)]_{\rm loc} = \frac{2}{g^2} \sum_{i=1}^{2(d-1)} \mathrm{Re}\,\mathrm{Tr}\left[\mathbb{I} - U_\mu(n) P_i\right] = \frac{2}{g^2}\,\mathrm{Re}\,\mathrm{Tr}\left[2(d-1)\mathbb{I} - U_\mu(n) A\right] , \tag{32}$$

where P_i is the contribution of the i-th plaquette without the link being tested and A is the sum of such "staples"

$$\begin{aligned} A = \sum_{i=1}^{2(d-1)} P_i = \sum_{\nu\neq\mu} \big(& U_\nu(n+\hat\mu) U_{-\mu}(n+\hat\mu+\hat\nu) U_{-\nu}(n+\hat\nu) \\ & + U_{-\nu}(n+\hat\mu) U_{-\mu}(n+\hat\mu-\hat\nu) U_\nu(n-\hat\nu) \big) . \end{aligned} \tag{33}$$

The change in the action is

$$\Delta S = S[U_\mu(n)']_{\rm loc} - S[U_\mu(n)]_{\rm loc} = -\frac{2}{g^2}\,\mathrm{Re}\,\mathrm{Tr}\left[(U_\mu(n)' - U_\mu(n)) A\right] . \tag{34}$$

Since the computation of the products of gauge group is by far the most time consuming part of the program, it is convenient to perform many proposal and acceptance test on the same link variable before moving to the next one. We compute the sum of staples just once and then by iterating the Metropolis algorithm, we have more chances that the link variable is changed, and the configuration space is thus better spanned. This *multi-hit Metropolis algorithm* have been performed with $5 \div 10$ repetitions, depending on the simulation. In the limit of infinite repetitions one should recover the results of the heat bath algorithm, presented in the next section. In this way also effects due to correlations are somehow reduced.

An important parameter of the simulation is the acceptance ratio, that is the ratio of the accepted single link Metropolis updates over the total proposed ones. A too small acceptance ratio would be costly, since many configurations would be proposed but not accepted, while a too high acceptance ratio means too small changes in the action and leads to slow motion in configuration space and high correlations. Usually one tries to keep the acceptance ratio around 0.5, which is a reasonable compromise. To control the acceptance ratio, we introduce a parameter ϵ in the choice of the proposed new link variable. New link variables cannot be too far from the previous ones, otherwise they will

never be accepted. The idea is to generate a random group element $X(\epsilon)$ close to the unity element and multiply the old link variable with this random matrix, $U_\mu(n)' = X(\epsilon)\, U_\mu(n)$. The parameter ϵ controls how much the matrix X is close to unity. For example, for $SU(2)$ matrices, one can generate a random number r between 0 and ϵ, and three random numbers b_i in the interval $(-1/2, 1/2)$. Then $a_i = \epsilon/|\vec{b}|^2$ and $a_0 = \sqrt{1-\epsilon^2}$. Random $SU(3)$ matrices close to $\mathbb{I}_3$ are generated starting from embedded random $SU(2)$ matrix, while a random $U(1)$ phase is simply found by generating a random $\phi \in (\epsilon, \epsilon)$ and setting $X = (1 + i\phi)/\sqrt{1+\phi^2}$.

Below is reported a schematic version of the code used for the implementation the Metropolis sweep.

```
for (site_index = 0; site_index < Nsite; ++site_index) {
  /*  get lattice vector n from site index */
  n = get_lvector(site_index);

  for (mu = 0; mu < dimension; ++mu) {
    /*  get gauge field to be modified and compute the sum of staples */
    U = gauge_field.at(site_index).at(mu);
    A = computeStaples(n, mu);

    /*  perform the Metropolis move */
    for (i = 0; i < trials; ++i) {
      proposal++;
      X.random(eps);
      U_candidate = X * U;
      DeltaS = - 2./(g2) * ( (U_candidate - U) * A ).getReTr();
      if ( DeltaS <= 0. ) {
        gauge_field.at(site_index).at(mu) = U_candidate;
        U = U_candidate;
        accepted++;
      } else {
        R = rand0to1();
        if ( R < exp(-DeltaS) ) {
          gauge_field.at(site_index).at(mu) = U_candidate;
          U = U_candidate;
          accepted++;
        }
      }
    } /* for cycle on metropolis trials */
  } /*   for cycle on directions      */
} /*     for cycle on sites           */
acceptance_ratio = accepted / proposal;
```

2.4 The Heat Bath algorithm for SU(2)

In the heath bath algorithm one directly generates the new link variable $U_\mu(n)'$ according to the local probability distribution defined by the surrounding staples

$$\mathrm{d}P(U) = \mathrm{d}U \, \exp\left(\frac{2}{g^2} \mathrm{Re}\,\mathrm{Tr}[U\,A]\right) . \tag{35}$$

Notice that $\mathrm{d}U$ is the Haar measure and in general it is not possible to generate new link variables in such a way. However, for the gauge group $SU(2)$ there is a simple way to implement the heat bath algorithm. The payback is that the correlations are reduced with respect to the Metropolis case, since the new link variable will be independent from the old one (we are not proposing a new group element close to the previous one), and the links are updated very efficiently since the link variable always changes (there is no acceptance test).

What allows an efficient heat bath algorithm is the fact that the sum of two $SU(2)$ matrix is proportional to another $SU(2)$ matrix, the proportionality constant being the determinant of the matrix. In this way the sum of staples can be written as

$$A = a\,V \qquad \text{with} \qquad a = \det A\,, \quad V \in SU(2)\,. \tag{36}$$

If we define the $SU(2)$ matrix $X = UV$, we can write the local probability distribution for X

$$\mathrm{d}P(X) = \mathrm{d}X \, \exp\left(\frac{2}{g^2} a\,\mathrm{Re}\,\mathrm{Tr}[X]\right) , \tag{37}$$

where the Haar measure is simply given by $\mathrm{d}X = \frac{1}{\pi^2}\mathrm{d}^4x\,\delta(x_0^2 + |\vec{x}|^2 - 1)$. Going to polar coordinates in $(x_0, \vec{x})$, using standard formulas for the δ-function and remembering that $\mathrm{Tr}\,X = 2x_0$, an elementary calculations leads to

$$\mathrm{d}P(X) = \frac{1}{2\pi^2}\mathrm{d}\cos\theta\,\mathrm{d}\varphi\,\mathrm{d}x_0\,\sqrt{1-x_0^2}\;e^{\frac{2}{g^2}a\,x_0} . \tag{38}$$

The pdf for the variables x_0, θ and φ factorize while $|\vec{x}|^2$ has already been integrated out and it is fixed to one. There are standard ways to draw a random variable from an exponential distribution such as $e^{\frac{2}{g^2}a\,x_0}$. This variable is then accepted with an accept/reject step with the probability given by the square root $\sqrt{1-x_0^2}$. The variables x_i are generated uniformly on the unitary 3-dimensional sphere.

A possible (pseudo)code to implement these ideas is reported below. It has been used for the simulations regarding the $SU(2)$ gauge group.

```
for (site_index = 0; site_index < Nsite; ++site_index) {
  /*  get vector n from site index */
  n = get_lvector(site_index);

  for (mu = 0; mu < dimension; ++mu) {
    /* compute the sum of staples relative to the tested gauge field */
    A = computeStaples(n, mu);
    a = sqrt( ( A(0,0)*A(1,1) - A(0,1)*A(1,0) ).Re );

```

```
10      if (a == 0.) { /* if detA=0, get a random SU(2) element */
11        for (i = 0; i < 4; ++i) x.at(i) = 2.*rand0to1() - 1.;
12        Unew = SU2matrix(x);
13        gauge_field.at(site_index).at(mu) = Unew;
14      } else {
15        /*  compute V */
16        v.at(0) = ( A(0,0).Re ) / a;
17        v.at(1) = ( A(0,1).Im ) / a;
18        v.at(2) = ( A(0,1).Re ) / a;
19        v.at(3) = ( A(0,0).Im ) / a;
20        V = SU2matrix(v);
21
22        do {/* generate x0 */
23          r1 = 1. - rand0to1();
24          r2 = 1. - rand0to1();
25          r3 = 1. - rand0to1();
26          lambda2 = -(g2/(a*8.))*( log(r1) + cos(2.*PI*r2)*cos(2.*PI*r2)*log(r3) );
27          r = rand0to1();
28        } while ( (r*r) > (1.-lambda2) );
29
30        x.at(0) = 1. - 2.*lambda2;
31
32        do { /*  generate x1, x2, x3 uniformly distributed in the 3-sphere of
                radius \sqrt{1-x_0^2} */
33          r1 = 2.*rand0to1() - 1.;
34          r2 = 2.*rand0to1() - 1.;
35          r3 = 2.*rand0to1() - 1.;
36          rsquare = r1*r1 + r2*r2 + r3*r3;
37        } while ( rsquare > 1. );
38
39        norm = sqrt( (1. - x.at(0)*x.at(0)) / rsquare );
40        x.at(1) = r1 * norm;
41        x.at(2) = r2 * norm;
42        x.at(3) = r3 * norm;
43
44        /*  get new link variable */
45        X = SU2matrix(x);
46        Unew = X * V.getInverse();
47        gauge_field.at(site_index).at(mu) = Unew;
48      }
49
50    } /* for cycle on directions */
51  } /*   for cycle on sites    */
```

2.5 Measurements and analysis

As already mentioned, I concentrated on the determination of the parameter σ discussed in sec. 1.4. This parameter can give strong hints on the presence or absence of confinement, even in the absence of dynamical charged fermions.

In order to extract the value of σ from the numerical calculations, Monte Carlo averages of Wilson loops or Polyakov loops have been computed. To have a better statistics, we need to compute the average over all Wilson loops of the lattice with time extension $t = n_t a$ and spatial extension $r = n_r a$ (actually, due to rotational invariance, all Wilson loops in any fundamental plane of the lattice can be taken into account, even in the pure spatial planes). For the same reason all possible products of Polyakov loops at a given distance r have been averaged out.

We discussed in sec. 1.4 that in the infinite lattice temporal size both Polyakov loops and Wilson loops can be parametrized in terms of the static $q\bar{q}$ potential $V(r)$

$$\langle W[U] \rangle \sim e^{-n_t \hat{V}(r)} , \qquad \langle P(\vec{m}) P(\vec{n})^\dagger \rangle \sim e^{-N_t \hat{V}(r)} \tag{39}$$

If we compute the Wilson or Polyakov loops for different values of r we can study the behavior of the potential. If we parametrize the potential as in eq. (21), we can recover the various parameters from a fit of the computed data.

Actually, a problem that one encounters is the fact that sometimes the exponential behavior found in eq. (39) makes the values of the Wilson and Polyakov loops very small and statistically indistinguishable from zero. For small values of the inverse coupling $\beta = 2N/g^2$, often only loops of dimension up to 2 lattice links or even 1 (that is the fundamental loop, the plaquette) are sensibly different from zero. In this case a fit is impossible since we have too few points. To overcome the problem, we can add a point setting $\langle W \rangle = 1$ for $r = 0$ (that is $V(0) = 0$) or we can assume a pure linear behavior in the potential, thus reducing the number of unknown parameters to just one, that is σ (remember that the strong coupling expansion indeed shows that in this regime the linear contribution is the leading one). This techniques have proven to give good results, despite their intrinsic ambiguity.

For a more detailed discussion of the numerical techniques used to simulate pure gauge theories, see [2].

3 Results and discussion

3.1 $U(1)$ symmetry

The $U(1)$-symmetric, 2-dimensional case can be solved analytically [3]. The expectation value of the Wilson loop can be computed exactly. Indeed, since the gauge group is Abelian, the Wilson loop can be replaced by the product of the single plaquettes enclosed in the loop. Let us call U_P the product of the link variable around the plaquette P

$$\langle W_{\mathcal{L}(r,t)} \rangle = \frac{\int \mathcal{D}U \left(\prod_{P \in \mathcal{L}} U_P \right) e^{\frac{\beta}{2} \sum_P (U_P + U_P^\dagger)}}{\int \mathcal{D}U \, e^{\frac{\beta}{2} \sum_P (U_P + U_P^\dagger)}} . \tag{40}$$

Exploiting the gauge symmetry, we can fix the gauge in such a way that the link variables along the time direction are set to one. The plaquette reduces to

$$U_P = e^{i\theta_P} , \qquad \theta_P = \theta_1(n_0, n_1) - \theta_1(n_0 + 1, n_1) . \tag{41}$$

With a change of variables, the integral can be rewritten in terms of θ_P

$$\langle W_{\mathcal{L}(r,t)} \rangle = \prod_{P \in \mathcal{L}} \frac{\int_{-\pi}^{\pi} \mathrm{d}\theta_P \, e^{i\theta_P} \, e^{\beta \cos\theta_P}}{\int_{\pi}^{\pi} \mathrm{d}\theta_P \, e^{\beta \cos\theta_P}} \,. \tag{42}$$

The integral is easily computed in terms of modified Bessel functions

$$\langle W_{\mathcal{L}(r,t)} \rangle = \left(\frac{I_1(\beta)}{I_0(\beta)} \right)^{n_r n_t} \,, \tag{43}$$

and the result is that the potential is linear in n_r, with

$$\hat{V}(n_r) = -\lim_{n_t \to \infty} \frac{1}{n_t} \ln \langle W_{\mathcal{L}(r,t)} \rangle = \hat{\sigma} n_r \,, \qquad\qquad \hat{\sigma} = \ln \left(\frac{I_0(\beta)}{I_1(\beta)} \right) \,. \tag{44}$$

The 2 dimensional Abelian theory is confining, even in the continuum limit. Such limit can indeed be taken simply studying the naive one. The coupling constant g has the dimension of a mass and therefore one is led to define the dimensionful coupling constant $e = \frac{1}{a} g$. By requiring e to be finite in the continuum limit, then $\beta = 1/(e^2 a^2)$ must diverge and considering the asymptotic expansions of the modified Bessel functions for large β one can see that the naive limit $a \to 0$ immediately gives finite physical results and the potential still grows linearly with the distance

$$V(r) = \frac{1}{2} e^2 r \,. \tag{45}$$

This example is not very illuminating, since many of the features of the generic lattice gauge theories are not present, such as a transition between confining and non-confining phase or a non-trivial RG flow. nevertheless it gives the chance to test the predictions of the simulation in a case where the exact analytic result is known. Fig. 1 shows the numerical result together with the exact one of eq. (44).

The situation changes drastically if we study the system in 4 dimensions (quenched QED). Large and small β expansions show that the system has two different phases: confining and non-confining. This is in agreement with the fact that in the continuum QED is known to be non-confining. The numerical computation confirmed what expected, the results are shown in fig. 2. In the non-confining phase the potential decreases with the distance. It is therefore possible to separate the $U(1)$ charges and to see free charged states. The potential for certain values of the parameter β is shown in fig. 3.

3.2 $SU(2)$ symmetry

The analysis for the $SU(2)$ symmetry can be done quite efficiently thanks to the heat bath algorithm. No phase transition is found and the theory is confining probably for all values of β. In fig. 4 the results for the string tension are reported. The scaling window is clearly visible and the fit in that region with the one-loop result of RG gives an estimate for $\hat{C}_\sigma$ that can be used to find Λ_L, once compared with the experiments. These results coincide with the one found by [4].

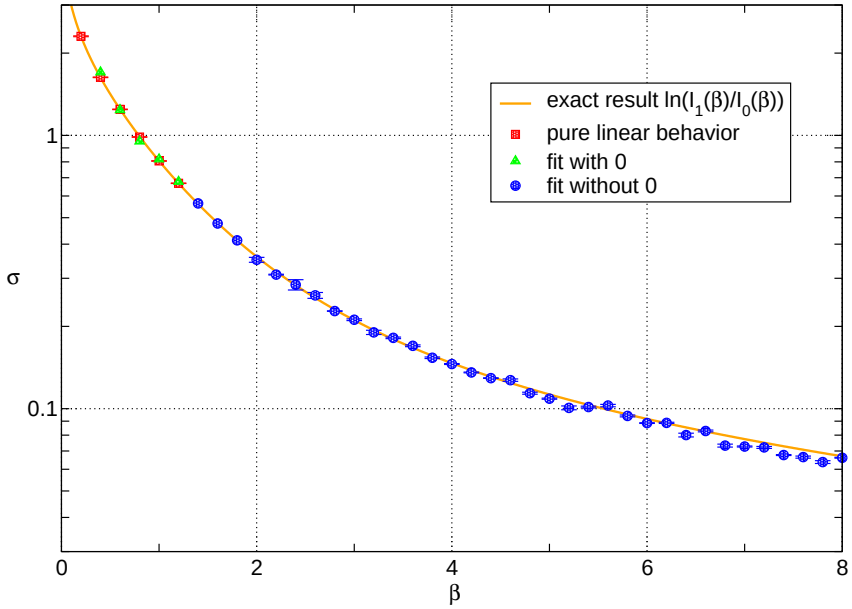

Figure 1: String tension for the $U(1)$ gauge symmetry in 2 dimensions. The agreement of the numerical data (obtained on a lattice with $N_s = 30^2$) with the exact analytical result is satisfying.

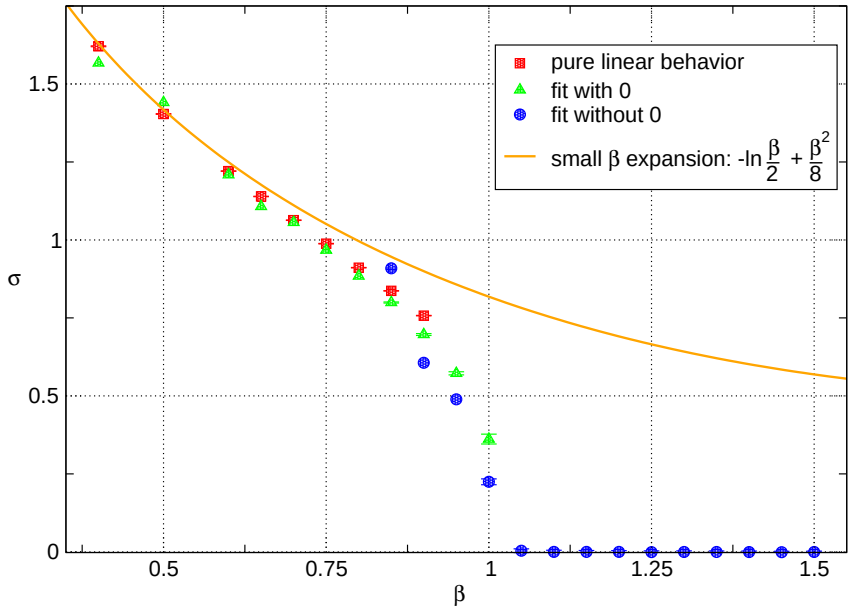

Figure 2: String tension for the $U(1)$ gauge symmetry in 4 dimensions. The data are taken from a lattice with $N_s = 9^4$. The confining phase ($\sigma \neq 0$) and the non-confining one ($\sigma = 0$) are clearly present. The analytical result valid for small β is also shown for comparison.

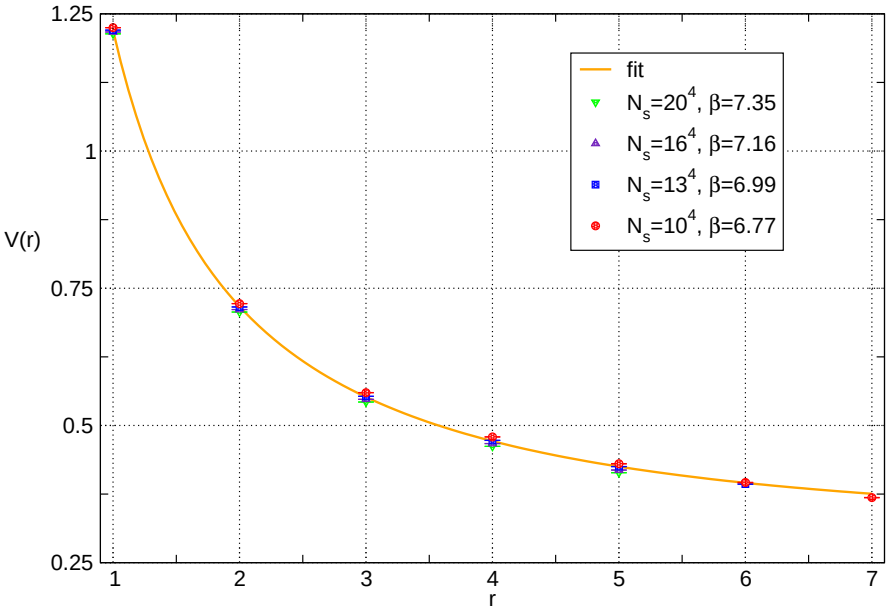

Figure 3: Potential for the $U(1)$ gauge symmetry in 4 dimensions for some value of the parameter β in the non-confining phase. The data are taken from a lattices with varying lattice dimensions, such that the physical dimension is essentially the same in all cases. The potential tends to zero for large distances. The fit is performed with the data with $\beta = 6.99$. The fit gives $\sigma \sim 0$, $A \sim 0.2$ and $B \sim 1$, in terms of the parametrization of eq. (21).

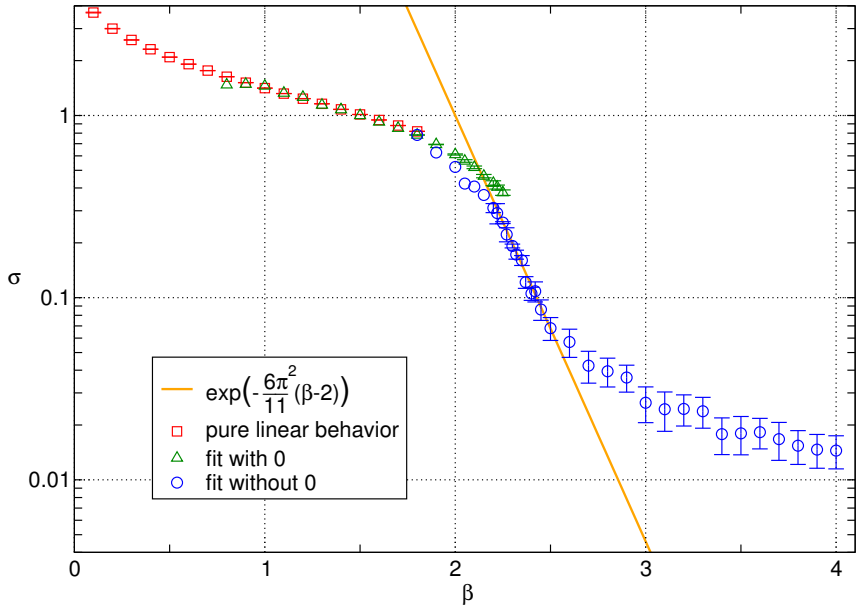

Figure 4: String tension for the $SU(2)$ symmetric case on a lattice with $N_s = 9^4$. The analysis was performed with the heat bath algorithm.

3.3 $SU(3)$ symmetry

For the $SU(3)$ case the computational effort grows a lot, compared with the two previous cases. Only a few values of β have been considered and the lattice extension was tuned according to (27) in such a way that the physical space-time dimensions were almost constant. The potential is shown in fig. 5.

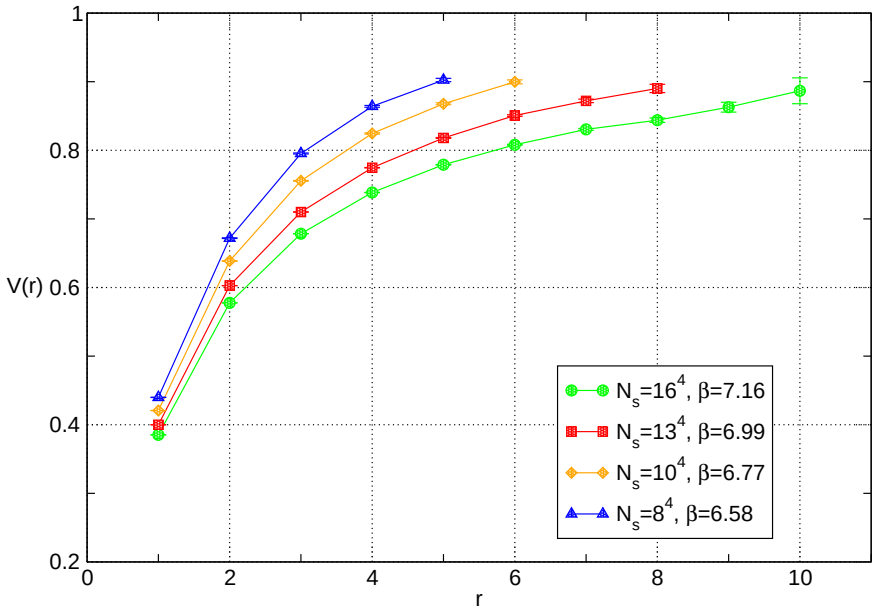

Figure 5: Potential for the $SU(3)$ gauge symmetry in 4 dimensions for some value of the parameter β. Lines are drawn just to guide the eye. The data are taken from a lattices with varying lattice dimensions, such that the physical dimension is essentially the same in all cases. The potential is found to grow linearly for large distances.

With the chosen values of β we should already be in the scaling region, so we expect σ to scale as in eq. (28). The analysis is shown in fig. 6, where we fit the data with the one- and two-loop result for the function $R(\beta)$. Actually the fit is not very precise (and the error bars are very large if compared with the difference in subsequent points), probably with a larger statistics (which would require an optimization of the computer program) a better result may be found. Some improvement can also be obtained taking into account more terms in the loop expansion (which is actually valid for small β). Despite the poor result, confinement is clearly present.

3.4 Z_n symmetry

Not only continuous gauge symmetries, discrete gauge symmetries can be studied as well on the lattice. We concentrated on the Z_2 case, for which a simple implementation of the heat bath algorithm is possible.

It is possible to show that in two dimension the Z_2 lattice gauge theory can be mapped

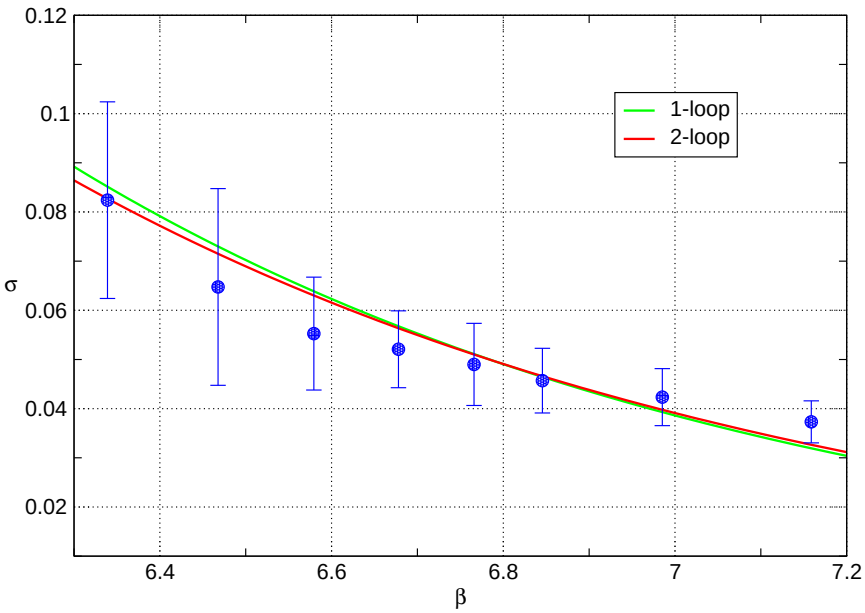

Figure 6: String tension for the $SU(3)$ gauge symmetry in the scaling region, obtained from the fit of the data shown in fig. 5. The one- and two-loop result for the scaling relation cannot approximate very well the numerical data in this regime.

onto the 1-dimensional Ising model (see for example [5]). As it is well known, this model does not show any symmetry breaking. This is indeed what the simulation also found, the result is shown in fig. 7.

Things change when we consider the 3-dimensional Z_2-invariant lattice. If we consider different couplings β_t and β in the time and space directions, we can take the limit of continuous time by simultaneously taking

$$\beta_t \to \infty\,, \qquad \beta \to \lambda e^{-2\beta_t}\,. \tag{46}$$

This fact can be seen using the transfer matrix formalism. In this limit, the system can be mapped onto the 3-dimensional Ising model with temperature λ^{-1} (a proof of this statement can again be found in [5]). This model is known to show a second order phase transition for some critical value λ_c^{-1}. Therefore we expect the 3 dimensional Z_2 lattice gauge theory to show a phase transition as well. This is indeed what was found from the numerics, the results are shown in fig. 8 and 9, where the transition is clearly present. In fig. 10 the thermalization for different values of β above and below the critical point are shown. The effect of critical slowing down is present around the transition.

In our simulations we kept the same coupling constant both in the time and space directions. The correspondence with the 3-dimensional Ising model and the relations of eq. (46) are true only in the limit of continuous time. However, we can forget for a moment about this and pretend that the gauge theory is equivalent to the 3-dimensional Ising model at temperature $\lambda^{-1} = \beta^{-1}e^{-2\beta_t}$ for any value of β and β_t. In this case, given that the critical value at which we found the transition is $\beta_c \sim 0.74$ ($\beta = \beta_t$ in our simulation) we can

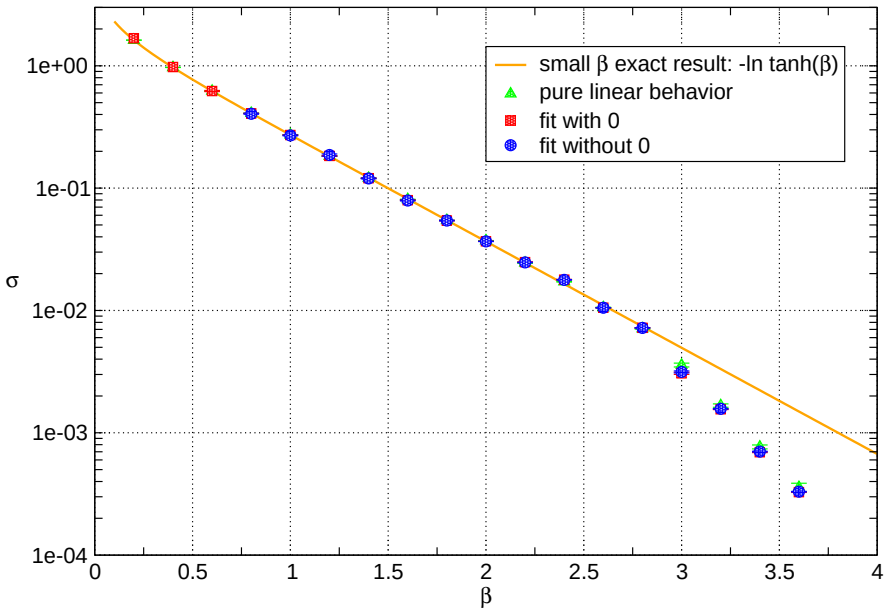

Figure 7: String tension for the Z_2 gauge symmetry. The data are taken from a lattice of dimension $N_s = 80^2$. No transition is present. The analytical result of the small β expansion is also shown.

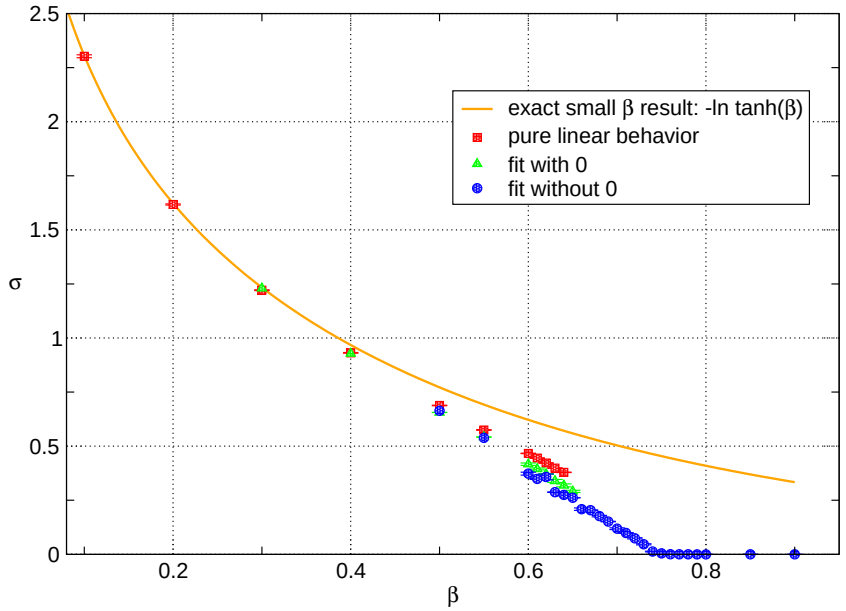

Figure 8: String tension for the 3-dimensional Z_2 lattice gauge theory. The transition is clearly present. Data are obtained from a lattice of dimension $N_s = 20 \times 20$. The small β expansion is also shown.

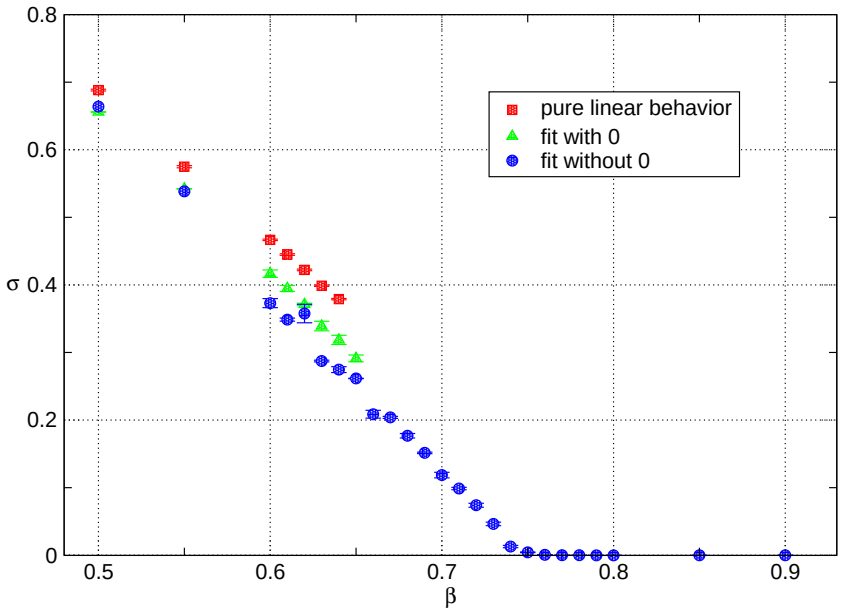

Figure 9: Detail of fig. 8 around the critical point. The transition is found for $\beta \sim 0.74 \div 0.75$.

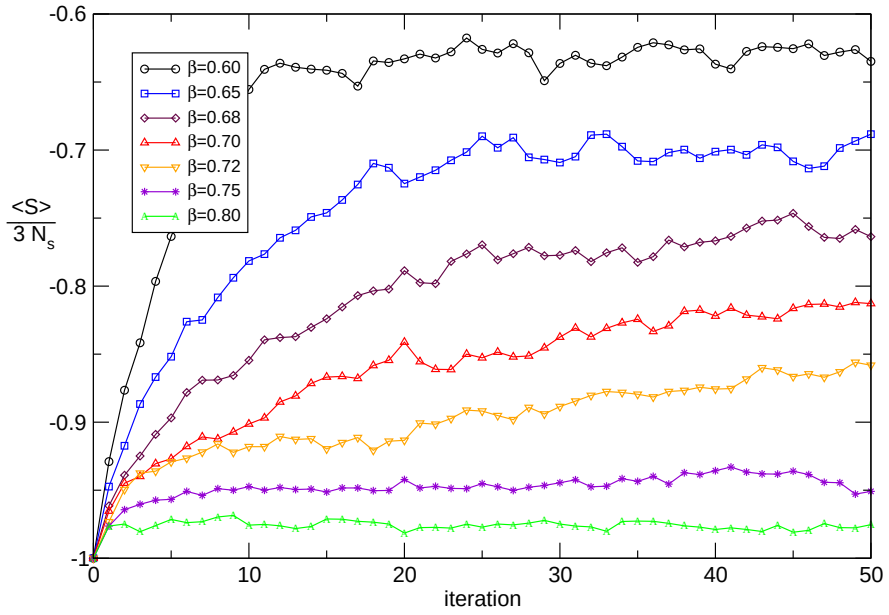

Figure 10: Thermalization for the 3-dimensional Z_2 gauge theory for different values of β above and below the critical point. Thermalization is much slower in the vicinity of the transition (critical slowing down).

get the critical value for the Ising model, namely $\lambda_c^{-1} = \lambda_c^{\text{Ising}} \approx 0.308$. With this critical value and exploiting again the relation between λ and β (this time for the values of the Ising model), that is $\lambda^{\text{Ising}} = \beta^{\text{Ising}} e^{2\beta^{\text{Ising}}}$, we can find the critical value of the inverse temperature for the Ising model $\beta_c^{\text{Ising}} \approx 0.204$. Despite the very crude approximations, motivated by presumably wrong assumptions, the value that we find is only within a 10% from the true critical inverse temperature $\beta_c^{\text{Ising}} = 0.222$. However, only a better investigation, independently varying the coupling constants in time and space directions may possibly confirm that this result is somehow well-grounded.

3.5 Finite temperature

We can also study the system at thermal equilibrium at finite temperature. The partition function for a general quantum mechanical system with Hamiltonian $\widehat{H}$ at temperature T is given by

$$Z(T) = \text{Tr}\left[e^{-\beta_T \widehat{H}}\right] , \tag{47}$$

where β_T is the inverse temperature $\beta_T = 1/(k_B T)$ and must not be confused with the inverse of the gauge coupling constant (from now on we will consider $k_B = 1$). With the standard Suzuki-Trotter decomposition we can transform the partition function in a path integral over field configurations. The result will be identical to the one of the dynamical theory at zero temperature. However we are now assuming to be at equilibrium, therefore the fields will not have any time dependence and the role of the time is now played by the inverse temperature β_T. We do not assume an infinite time extent of the system, instead we consider a finite extent, with the upper value related to the finite inverse temperature. The partition function can be written as follows

$$Z(T) = \int \mathcal{D}U \, e^{-S_E[U]} , \tag{48}$$

with

$$S_E[U] = \int_0^{\beta_T} \mathrm{d}t \int_{\mathbb{R}^3} \mathrm{d}^3x \, \mathcal{L}(U(t,\vec{x}), \partial_\mu U(t,\vec{x})) . \tag{49}$$

We see that the program used so far can be used also to study the system at equilibrium at finite temperature. Only the interpretation of the results will change. An important point is that in the zero temperature analysis we were interested in the results for the infinite space-time volume limit, in the sense that we needed space-time extents larger than the correlation lengths of the system. In this new perspective space is still considered in this limit, while the physical extent of time (which must interpreted as the inverse temperature) is limited to β_T. For a finite lattice the space extent is aN while the time extent is $aN_T = \beta_T = 1/T$. The continuum limit corresponds to $a \to 0$ while holding the physical spatial extent aN and the inverse temperature aN_T fixed. Finite size effects will decrease for large value of the ratio N/N_T, therefore for the simulation we should consider lattices with time extension smaller than the spatial one.

We are interested in looking for a confinement-deconfinement transition driven by the temperature. Such a transition is a fundamental issue for many physical problems, as for example the early phases after the big bang and the physics of neutron stars or other

astronomical compact objects. To study this transition we will focus on Polyakov loops. We argued that the correlator between two Polyakov loops is related to the free energy of a pair of static quark and antiquark according to

$$\langle P(\vec{m})P(\vec{n})^\dagger\rangle = e^{-aN_T F_{q\bar{q}}(a|\vec{m}-\vec{n}|)} = e^{-F_{q\bar{q}}(r)/T}\,. \tag{50}$$

At large distances we expect factorization

$$\lim_{a|\vec{m}-\vec{n}|\to\infty}\langle P(\vec{m})P(\vec{n})^\dagger\rangle = |\langle P\rangle|^2\,, \tag{51}$$

where the spatial dependence of the lhs can be dropped thanks to translational invariance and the spatial average may be considered. When the theory is confining, if the two quarks are taken far apart then $F_{q\bar{q}}$ must grow indefinitely and therefore $\langle P\rangle$ must vanish. On the contrary, if the theory is not confining, $\langle P\rangle$ is finite

$$\begin{aligned} &\langle P\rangle = 0 \qquad \Leftrightarrow \qquad \text{confinement} \\ &\langle P\rangle \neq 0 \qquad \Leftrightarrow \qquad \text{no confinement}\,. \end{aligned} \tag{52}$$

We can also interpret the expectation value of a single Polyakov loop as the probability to observe a single static charge

$$|\langle P\rangle| \sim e^{-F_q/T}\,. \tag{53}$$

If the theory is confining F_q is infinite, while if it is not confining F_q is finite.

Since $T = 1/(N_T a)$, in order to study the system at different temperatures we can vary the lattice extent in the "time" direction N_T, or we can vary the lattice spacing a by tuning the gauge coupling constant $\beta = 2N/g^2$. When β increases the lattice spacing a decreases and therefore T increases. To set the scale of temperatures one should study the scaling of some observables and compare it with some experiment, thus fixing the value of Λ_L and hence a[5].

In fig. 11 we plot the modulus of the expectation value of the Polyakov loop for the $SU(3)$ symmetric lattice gauge theory. The transition is clearly present and a detailed study of the physical dimensions of the system would fix the critical temperature to $T_c \approx 270\,\text{MeV}$. This transition has been widely studied and it was found to be weakly first order.

The finite temperature transition in quenched QCD coincides with the spontaneous symmetry breaking of the center symmetry of the gauge group $SU(N)$, that is Z_N. This can be seen from the Polyakov loops. Indeed if we perform a center transformation, that is a gauge transformation where all gauge elements of the temporal links of a time slice are multiplied by an element of the center $U_0(t_0,\vec{n}) \to zU_0(t_0,\vec{n})$, the action is invariant while the Polyakov loops will be multiplied by this center element. This is due to the fact that the action is computed as the sum of trivially closed loops and any of such loops will not be affected by a center transformation. Indeed any trivially closed loop with a component in the time direction will be multiplied by z when the loop crosses the time slice the first time and by its conjugate z^* when it comes back and crosses the time slice

[5] Analogously one could use the Sommer parameter to find the physical value of the lattice spacing a (for a definition of the Sommer parameter and a discussion about how to use it to fix the physical scale, see for example the discussion in [2]).

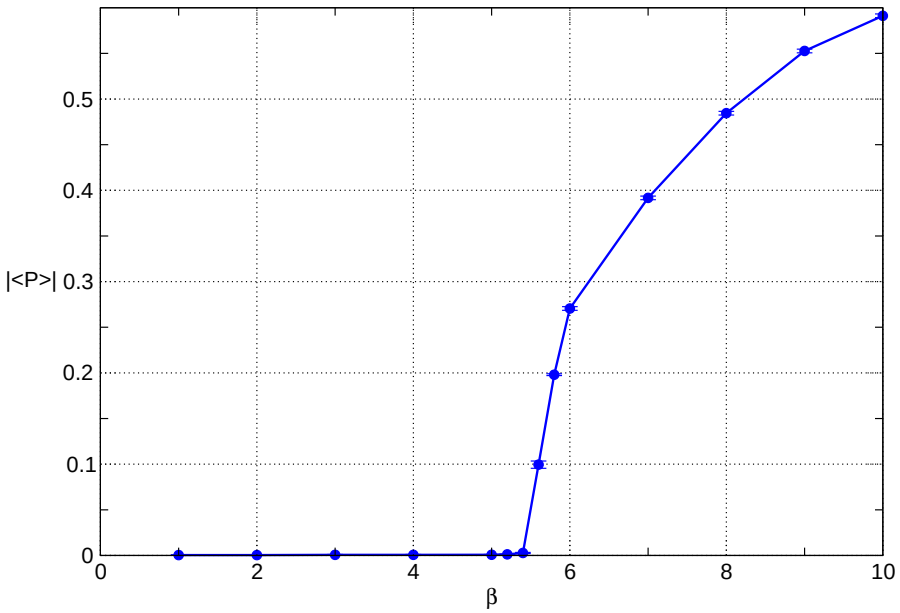

Figure 11: Modulus of the expectation value of the polyakov loop $|\langle P\rangle|$ as function of the inverse coupling β. Increasing β means increasing temperature T. The simulation was performed on a lattice of dimension $N_s = 12^3 \times 4$.

for the second time in the opposite direction. Since the center elements commute with all elements of the gauge group, they cancel out from the loop. This is not true any more for the Polyakov loops, since they wind around the temporal direction and do not close trivially. They are multiplied just once times the center element and therefore they are not invariant $P \to zP$.

The expectation value of the Polyakov loop will be zero in the unbroken phase

$$\langle P\rangle = \frac{1}{N}\langle \sum_{n=0}^{N-1} z^n P\rangle = 0\,, \tag{54}$$

since the sum of the elements of the center Z_N is zero. We are in the confining phase. However this ends to be true in the broken phase, and P acquires a non-zero expectation value. Of course on a finite lattice we cannot have a true phase transition to a broken phase (an infinite volume is needed) and if we wait a large enough time, the system will tunnel from one phase to another, eventually spanning all the phase space and $\langle P\rangle$ is therefore forced to vanish. In our simple simulations, the simulation time was shorter than the persistence time of the system in a single phase, therefore we did not need to manually cure this problem. However, systematic errors due to tunneling are not under control in this way. To somehow avoid the problem one may plot $\langle |P|\rangle$ instead of $|\langle P\rangle|$, the former being unaffected by tunneling from one phase to another. The two values coincide in the infinite space limit.

Early studies of the Z_3 gauge spin model [6, 7] showed a first order phase transition, in agreement with the result for the finite temperature transition of $SU(3)$ QCD.

In fig. 12 we plotted in the complex plane the value of the Polyakov loop on single gauge configurations. Black dots refer to a system with $T < T_c$, which is in the unbroken, confining phase. Colored dots instead are computed at $T > T_c$, when the system is in the broken, non-confining phase. The values of P in the broken phase concentrate along the center phases. In order to get the latter points, three runs have been performed starting from a "cold" configuration with all link variables set to unity and performing a center transformation just before starting the thermalization. This led the Monte Carlo chain in the desired phase.

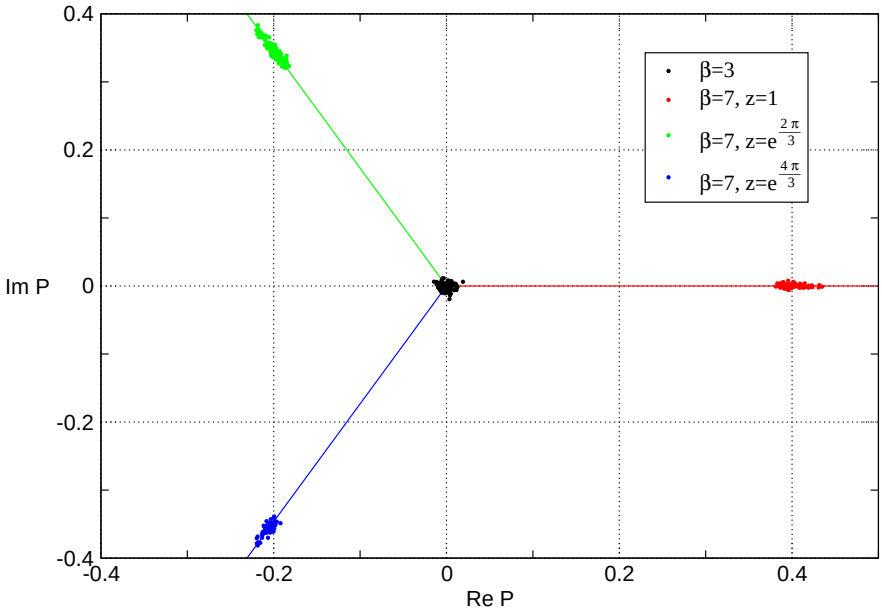

Figure 12: Polyakov loops in the complex plane on single gauge configurations. Black dots are computed in the unbroken phase (confining), $T < T_c$, while colored dots are computed in the broken phase (non-confining), $T > T_c$. The data are taken from a lattice of dimension $N_s = 12^3 \times 4$. For $T > T_c$ the system was driven in the desired phase by performing a center transformation right after the "cold" initialization.

4 Conclusions and possible improvements

The program has been tested in the case were the exact results were known and it gives correct results. In the other cases it gave results compatible with the one found in the literature. However, if a deeper analysis has to be done, more statistics is needed and the program needs to be improved to be faster. A better analysis of errors must be implemented too. Despite the various tricks used to lower the correlations, there is still no control on this point and errors are probably underestimated. A deeper analysis must be performed such that the correct estimation of the error could be found.

As it is, the program could be improved by adding a function to compute the hadron masses in the quenched approximation. The meson and baryon masses are computed from

the lowest energy states extracted from the correlators of meson and baryon interpolators (that is combinations of operators such as $\bar{q}\Gamma q$, where Γ is a combination of γ matrices). Recalling the fact that the fermion contribution to the action is quadratic, the average of a general observable O can be written as

$$\begin{aligned}\langle O\rangle &= \frac{1}{Z}\int \mathcal{D}U\, e^{-S_G[U]}\mathcal{D}[\psi,\bar{\psi}]\, e^{-S_F[\psi,\bar{\psi},U]}O[\psi,\bar{\psi},U] \\ &= \frac{1}{Z}\int \mathcal{D}U e^{-S_G}\frac{\int \mathcal{D}[\psi,\bar{\psi}]e^{-S_F[\psi,\bar{\psi},U]}O[\psi,\bar{\psi},U]}{\int \mathcal{D}[\psi,\bar{\psi}]e^{-S_F[\psi,\bar{\psi},U]}}\det[D_\psi] \\ &= \frac{1}{Z}\int \mathcal{D}U e^{-S_G}\langle O[\psi,\bar{\psi},U]\rangle_F \det[D_\psi]\,,\end{aligned} \tag{55}$$

where $Z = \int \mathcal{D}U e^{-S_G[U]}\det[D_\psi]$ and $D_\psi[U]$ is the Dirac and color operator in the action of the fermion ψ, such that $S_F \sim \bar{\psi}^{\,a}_{\alpha}(n) D^{\;a\;\;b}_{\alpha\;\;\beta}(n|m)\psi^{\;b}_{\beta}(m)$. When the observable O contains a product of the fermionic operators (as in the case of hadron interpolators), using Wick's theorem we can write $\langle O[\psi,\bar{\psi},U]\rangle_F$ as a combinations of fermion propagators D_ψ^{-1}. In the quenched approximation one neglects the contribution of the determinant and keeps only the fermionic dependence coming from the propagators[6]. Thus the path integral average is computed only on gauge configurations and with a pure gauge action. Therefore we must not change the Monte Carlo part of the algorithm, we only need to add a function which computes the propagators D_ψ^{-1}. This is not trivial, since we need an efficient way to invert the matrix D_ψ, but in principle it can be done.

Adding dynamical fermions is much more difficult. First of all we would need to introduce pseudofermions, that is bosons with the same number of degrees of freedom as femions, in order to deal with the quark fields. Then, when we reintroduce the determinant of eq. (55), we can put it back in the exponential and it will contribute to the action with a term $-\operatorname{Tr}\ln[D_\psi[U]]$. The action is not local any more and this makes things a lot more complicated. The Monte Carlo algorithms used so far, which change the action locally, are no longer efficients and they must be replaced with smarter hybrid algorithms, where both Molecular Dynamics and Monte Carlo techniques are used. This is not trivial at all and the program should be essentially completely rewritten.

References

[1] S. Elitzur, Phys. Rev. D 12, 3978 (1975)

[2] C. Gattringer, C. B. Lang, "Quantum Chromodynamics on the lattice", Springer, Lecture notes in Physics 788 (2010)

[3] J. Rothe, "Lattice gauge theories. An Introduction", World Scientific lecture notes in Physics - Vol. 74, 3 ed. (2005)

[4] M. Creutz, Phys. Rev. D 21, 2308 (1980)

[5] J. B. Kogut, Rev. Mod. Phys 51, 659 (1979)

[6] This approximation is somehow motivated by the so called hopping parameter expansion.

[6] M. Creutz, L. Jacobs, C. Rebbi, Phys. Rev. D 20, 1915 (1979)

[7] J. B. Kogut, R. B. Parson, J. Shigemitsu, D. K. Sinclair, Phys. Rev. D 22, 2447 (1980)